Identifying and quantifying the mechanism of electron beam induced damage and recovery in hydroxyapatite

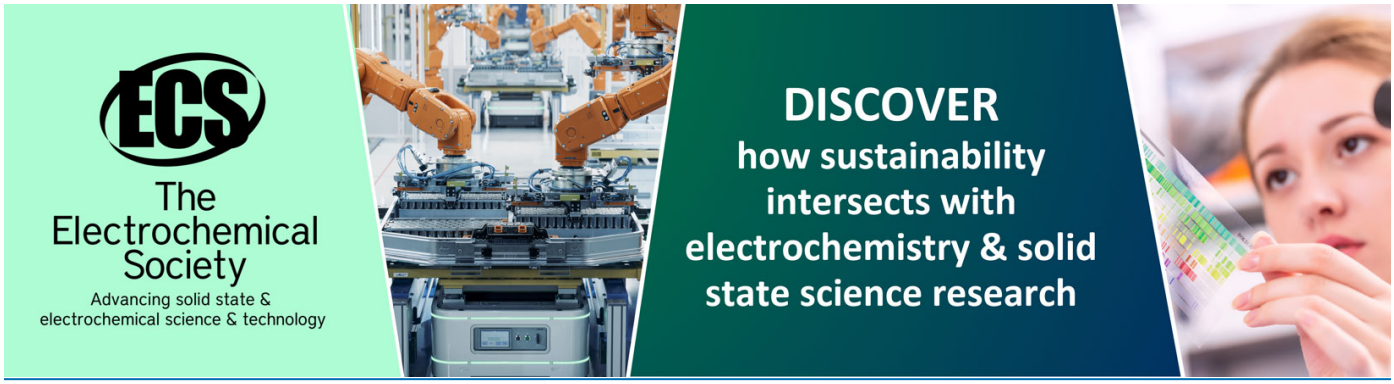

Journal of Physics: Conference Series **126** (2008) 012008 doi:10.1088/1742-6596/126/1/012008

Identifying and quantifying the mechanism of electron beam induced damage and recovery in hydroxyapatite

Patrick Eddisford, Andy Brown and Rik Brydson[1]
Institute for Materials Research, SPEME, University of Leeds, Leeds LS2 9JT, UK

E-mail: mtlrmdb@leeds.ac.uk

Abstract. Studies of electron beam induced damage in synthetic HA powder produced by standard solution-precipitation are reported. Under intense irradiation, such as that produced by a focused field emission source used when analysing a grain boundary or heterophase interface, it was found that the material damages transforming to cubic calcium oxide. The damage process was quantitatively monitored as a function of total fluence, fluence rate, accelerating voltage and specimen temperature by measuring the Ca/P ratio determined by EDX or EELS. Conclusions as to the exact damage and also recovery mechanisms in operation are drawn and the conditions required for limited-damage measurement are derived.

1. Introduction

Electron beam induced damage studies are a somewhat neglected aspect of electron microscopy particularly in the physical sciences. Many of the fundamental damage mechanisms were identified in the 1960s and 1970s [1]. However, since then, there have been significant improvements in both instrumentation, such as field emission sources and electron probe aberration correctors, and also in analytical methods, such as advances in the sensitivity and accuracy of energy dispersive X-ray analysis and also the emergence of electron energy loss spectroscopy as a powerful technique for both elemental and chemical analysis. Furthermore, with the rapid developments in bionanotechnology there are now significant research requirements for the high spatial resolution analysis of hybrid inorganic-organic nanostructured systems, either natural or synthetic. Such systems are amenable to study with analytical transmission electron microscopy if we seriously consider and quantify the nature and extent of electron beam induced damage under different experimental conditions [2].

Often authors use such vague phrases as “there was no visible change in the image or diffraction pattern during measurement”. However, quantification of the extent of damage from images or diffraction patterns is both difficult and rather insensitive and we have found that chemical signals such as energy dispersive X-ray (EDX) analysis or electron energy loss spectroscopy (EELS) are more sensitive and quantifiable. In particular, using EELS one can monitor relative sample thickness, elemental ratios, or electron loss near-edge structure (ELNES) [3] as a function of accumulated electron dose (or more properly fluence) or dose rate (fluence rate).

Hydroxyapatite (HA) is the mineral component in bone and tooth enamel with the nominal formula $Ca_{10}(PO_4)_6(OH)_2$. It is a highly significant biomaterial for applications such as biomedical ceramics and bioactive coatings for implants. With a view to the high spatial resolution analysis of not only HA

[1] To whom any correspondence should be addressed.

ceramic microstructures, but also HA incorporated in organic matrices such as tissue, we have begun preliminary investigations of the electron beam sensitivity of HA and report some interesting findings.

2. Experiment

Experiments were undertaken on both a high current density field emission gun TEM (FEI CM200) and also a lower current density (higher total current) thermionic LaB_6 TEM (FEI CM20) both operated at accelerating voltages between 80 and 200 kV. Qualitatively damage can be monitored by both bright field images and selected area electron diffraction patterns, however a more quantitative measurement of the extent of damage is provided by the (atomic) ratio of calcium to phosphorous (Ca/P) in the irradiated area as can be most conveniently measured by energy dispersive X-ray (EDX) analysis using an Oxford Instruments ultra thin window EDX detector (and ISIS processing software using virtual standards for the Ca and P Kα X-ray peaks) with a take off angle of 20° and a specimen tilt angle of 15°.

HA powder was obtained from Cambridge Materials (we acknowledge David Zhou and Serena Best) and also purchased from Sigma Aldrich (prepared by a solution-precipitation route). Based on the chemical formula, the Ca/P ratio in the undamaged material should be 1.66. However this is known to vary depending on the exact synthesis route and in the commercial Sigma Aldrich powder, the value was actually closer to 1.4. HA powder was ultrasonically dispersed in methanol and drop cast onto holey carbon support films. Aggregates of crystallites, which consisted of needles of diameter 10-20 nm and length ca. 100 nm, lying on the carbon support were analysed in order to reduce both charging and electron beam heating during irradiation.

Beam current was estimated by using an FEI calibration curve based on the measured brightness (i.e exposure time) on the (large) fluorescent TEM viewing screen: current (in nA) = 4.875/(Exposure Time for an emulsion setting of 2.0). The value derived from the calibration curve was independently checked by (indirectly) measuring the current incident on the drift tube of a Gatan Imaging filter with the spectrometer magnet switched off. Initial experiments were designed based on the commonly held assumption that damage in inorganic materials is principally a function of fluence (excluding hole drilling in, e.g. metal oxides which may also depend on fluence rate). Hence here total fluence (units electrons nm^{-2}) was altered by changing both the irradiation time and also the fluence rate (the setting of condenser 1, and hence beam current, and also the size of the irradiated area). However, later experiments were undertaken where fluence rate (units A cm^{-2}; note 1 A cm^{-2} = 624222 electrons nm^{-2} s^{-1}) was deliberately altered and measurements were taken at a set of different total fluences. Additional variables that were investigated were accelerating voltage (200, 120 and 80 kV respectively) and also the effect of cooling the sample via use of a liquid nitrogen cooled TEM holder.

3. Results

3.1. General effects of electron beam induced damage

At high fluences, it is observed in bright field images that HA needles change from an initial porous morphology (perhaps indicative of a hydrothermal processing route) to a less porous morphology with evidence of localized melting. This is accompanied by a concurrent change in the selected area electron diffraction pattern from that of hexagonal HA (ICDD reference 74-0565) to cubic calcium oxide (ICDD 00-037-1497) as shown in figures 1(b) and 1(c). This process is accompanied by a progressive increase in the Ca/P ratio (i.e. a loss of phosphorous which is also accompanied by a loss in oxygen) as determined by EDX or EELS. The EELS near edge structure (ELNES) at the O K-, Ca $L_{2,3}$- and P $L_{2,3}$-edges were found to progressively change with increasing fluence. These ELNES changes were consistent with formation of calcium oxide at high fluences as well as a change in the phosphorous chemical fingerprint from that of a phosphate to a phosphide or possibly elemental phosphorous. One possible explanation for this is an initial amorphisation of HA, loss of oxygen and phosphorous and then a subsequent recrystallisation in the beam to form crystalline CaO.

3.2. Initial experiments – damage as a function of fluence (whilst also varying fluence rate)

Figure 1(a) shows the Ca/P ratio as a function of fluence for current densities varying between 0.2 A/cm^2 and 24 A/cm^2 on the field emission TEM operating at 200 kV. It can be seen that above a total fluence of approximately 100 x 10^6 electrons nm^{-2}, the Ca/P ratio rapidly increases from the expected baseline value as damage progresses. Such a measurement was reproduced on both a field emission TEM and a LaB_6 TEM using similar, but not identical fluence rates. This initially suggested that fluence rates were not a critical factor in the damage process.

A further experiment was undertaken in which the sample was cooled to liquid nitrogen temperatures during measurement. Cooling was found to have only a small effect on the onset value of the fluence at which the damage process commenced (measured in terms of the Ca/P ratio) and surprisingly the onset of damage moved to slightly lower total fluences with cooling.

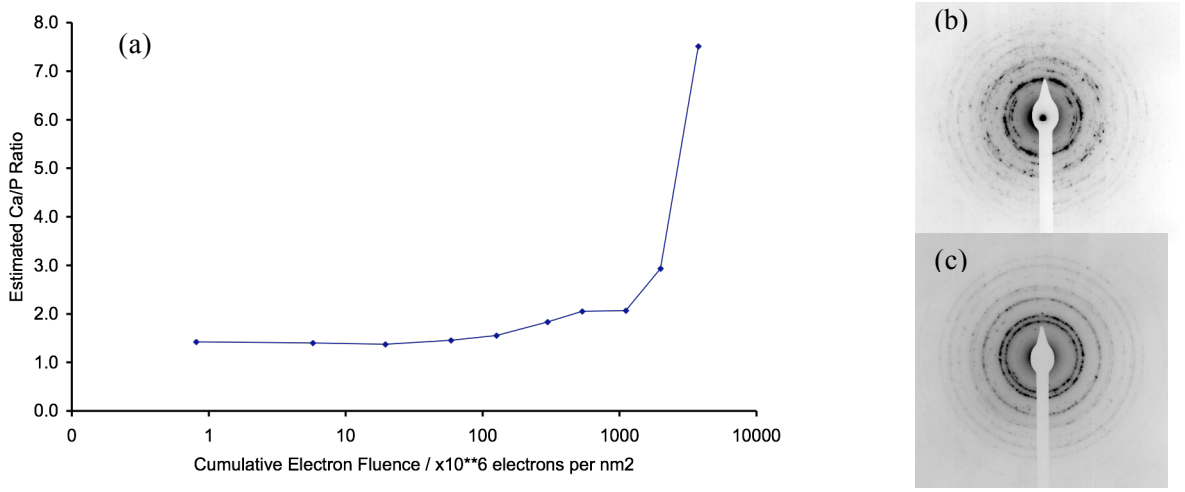

Figure 1. (a) EDX Ca/P ratio in HA plotted as a function of electron fluence. Selected area electron diffraction patterns at (b) low total fluence < ca. 10^8 electrons/ nm^2 and (c) high total fluence > 10^8 electrons/ nm^2.

3.3. Effect of accelerating voltage

Further measurements were undertaken on the LaB_6 TEM as a function of accelerating voltage. During these experiments the fluence rates were again varied so as to achieve progressively increasing electron fluences. However, for a given electron fluence, the fluence rates for the different accelerating voltages were broadly similar. Figure 2 shows a comparison of the Ca/P ratio as a function of electron fluence for 3 different accelerating voltages. Clearly the onset of damage (as measured by the Ca/P ratio) occurs at lower fluences as the accelerating voltage is lowered. Furthermore the data for the lower voltage experiments reveals a damage onset (possibly followed by a plateau), at higher fluences the damage subsequently increases. The increase in damage as the accelerating voltage is lowered is indicative of a damage process dominated by radiolysis (and ultimately specimen heating), owing to the increase in the ionization cross section. Unless there is an additional knock on mechanism in operation, there must also be a mechanism for converting the radiolytic energy acquired by atomic electrons in the sample to kinetic energy and momentum of atomic nuclei as there is an associated loss in crystallinity and also mass loss via removal of phosphorous and also oxygen. Strangely one would expect radiolysis to be reduced by cooling, which from the previous section appears not to be the case.

3.4. *Effect of fluence rate*

Some preliminary measurements at high fluence rates (current densities) ranging from 16 Acm^{-2} to 56 Acm^{-2} suggested that there was a significant dependence of the extent of damage at a particular total fluence on the fluence rate itself. This was investigated further at an accelerating voltage of 200 kV and figure 3 shows the dependence of the extent of damage on the fluence rate for a number of

different accumulated fluences between 150 x 10^6 and 1000 x 10^6 electrons nm^{-2}). As can be seen, for all accumulated fluences, at low fluence rates (ca. < 80 Acm^{-2}) damage actually decreases with an increase in fluence rate, there is then a distinct minimum and above this value the extent of damage is either constant or increases again. This behaviour is rather unexpected as most damage processes are assumed to be independent of fluence rate [2], and may be due to an uncorrelated recovery process [1] which is fluence rate dependent, i.e. it becomes activated only above a particular fluence rate.

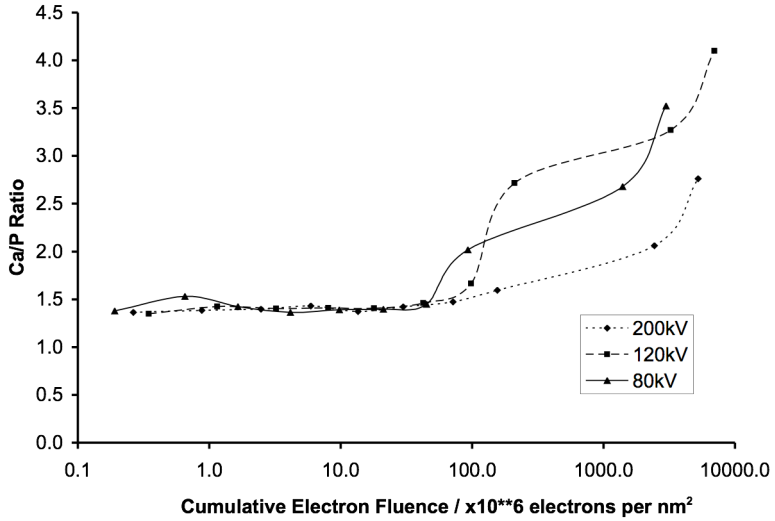

Figure 2. EDX Ca/P ratio in HA plotted as a function of electron fluence for three different accelerating voltages: 80, 120 and 200 kV.

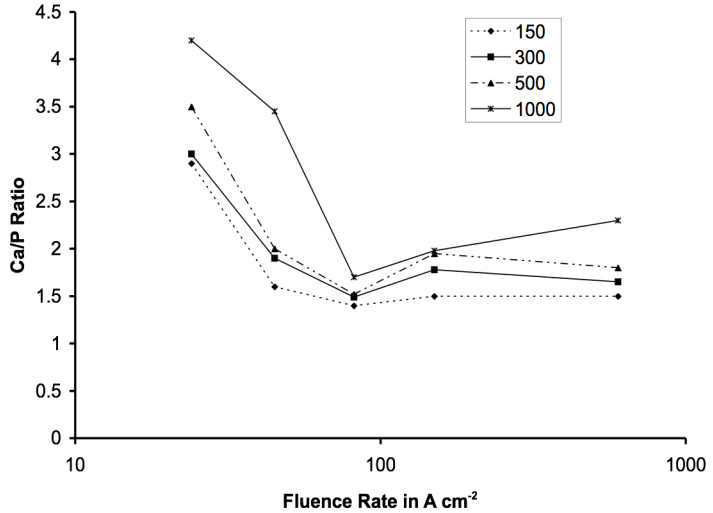

Figure 3. (a) EDX Ca/P ratio in HA plotted as a function of electron fluence rate (in Amps per cm^2) for four different total fluences : 150, 300, 500 & 1000 electrons nm^{-2} x 10^6.

4. Conclusions

This study of electron beam induced damage in HA has identified a radiolytic damage process involving loss of phosphorous and oxygen, amorphization and ultimately crystallization to form CaO occurring at fluences above 100x10^6 electrons nm^{-2} at 200 kV. The unexpected dependence of the damage process on fluence rate suggests a recovery process that becomes appreciable above a fluence rate of 80 Acm^{-2} (at 200 kV). This study hints at the importance of damage recovery processes in inorganic materials at high fluence rates which are readily achievable in field emission instruments.

5. References

[1] Hobbs L W in "Introduction to Analytical EM", p. 399-445, Plenum (1987).
[2] Egerton R F, Li P and Malac M, Micron 35 399-409 (2004).
[3] Sauer H, Brydson R, Rowley R et al., Ultramicroscopy 49, 198-209 (1993).